Icarus 357 (2021) 114266

Contents lists available at ScienceDirect

Icarus

journal homepage: www.elsevier.com/locate/icarus

Comprehensive investigation of Mars methane and organics with ExoMars/NOMAD

Elise W. Knutsen [a,b,*], Geronimo L. Villanueva [a], Giuliano Liuzzi [a,b], Matteo M.J. Crismani [c,d], Michael J. Mumma [a], Michael D. Smith [a], Ann Carine Vandaele [e], Shohei Aoki [e,f], Ian R. Thomas [e], Frank Daerden [e], Sébastien Viscardy [e], Justin T. Erwin [e], Loic Trompet [e], Lori Neary [e], Bojan Ristic [e], Miguel Angel Lopez-Valverde [g], Jose Juan Lopez-Moreno [g], Manish R. Patel [h,i], Ozgur Karatekin [j], Giancarlo Bellucci [k]

[a] NASA Goddard Space Flight Center, USA
[b] Department of Physics, American University, USA
[c] NPP/USRA, Goddard Space Flight Center, USA
[d] California State University, San Bernardino, USA
[e] Royal Belgian Institute for Space Aeronomy, Belgium
[f] University of Liege, Belgium
[g] Instituto de Astrofísica de Andalucía, IAA/CSIC, Spain
[h] School of Physical Sciences, The Open University, Milton Keynes, UK
[i] Space Science and Technology Department, Science and Technology Facilities Council, Rutherford
[j] Royal Observatory of Belgium, Belgium
[k] Istituto di Astrofisica e Planetologia Spaziali, Italy

ARTICLE INFO

Keywords:
Mars
Atmosphere
Methane
Infrared spectroscopy

ABSTRACT

Methane (CH_4) on Mars has attracted a great deal of attention since it was first detected in January 2003. As methane is considered a potential marker for past/present biological or geological activity, any possible detection would require evidence with strong statistical significance. Ethane (C_2H_6) and ethylene (C_2H_4) are also relevant chemical species as their shorter lifetimes in the Martian atmosphere make them excellent tracers for recent and ongoing releases. If detected, a CH_4/C_2H_n ratio could aid in constraining the potential source of organic production. Here we present the results of an extensive search for hydrocarbons in the Martian atmosphere in 240,000 solar occultation measurements performed by the ExoMars Trace Gas Orbiter/NOMAD instrument from April 2018 to April 2019. The observations are global, covering all longitudes and latitudes from 85°N to 85°S, and sampled from 6 to 100 km altitude with a typical vertical resolution of 2 km. There were no statistically significant detections of organics and new stringent upper limits for global ethane and ethylene were set at 0.1 ppbv and 0.7 ppbv, respectively. No global background level of methane was observed, obtaining an upper limit of 0.06 ppbv, in agreement with early results from ExoMars (Korablev et al., 2019). Dedicated searches for localized plumes at more than 2000 locations provided no positive detections, implying that if methane were released in strong and rapid events, the process would have to be sporadic.

1. Introduction

Mars has been characterized with ground-based observatories, Earth-orbiting telescopes, Mars orbiters, landers and rovers with increasing intensity since the pioneering studies of Mariner 4 in the mid 1960s. The ESA-Roscosmos spacecraft ExoMars Trace Gas Orbiter (TGO) is the first mission dedicated to measuring the vertical distribution of atmospheric trace gas composition on Mars (Vandaele et al., 2018). The Nadir and Occultation for MArs Discovery (NOMAD) instrument is part of the remote sensing suite of TGO, designed to observe the atmosphere in solar occultation, nadir and limb geometries to detect minor gaseous species (e.g., CH_4, H_2O, CO, O_3, HCl) and their isotopologues.

* Corresponding author at: NASA Goddard Space Flight Center, USA.
E-mail address: elisewrightknutsen@gmail.com (E.W. Knutsen).

https://doi.org/10.1016/j.icarus.2020.114266
Received 29 August 2020; Received in revised form 6 November 2020; Accepted 7 December 2020
Available online 15 December 2020
0019-1035/© 2020 Elsevier Inc. All rights reserved.

Determining the abundance or existence of methane and other organics would improve current photochemical models and provide novel insights into the astrobiological evolution of the planet (e.g., Atreya and Gu (1995)).

The atmosphere of Mars is heavily oxidized and primarily composed of CO_2 (95.3%), N_2 (2.7%) and Ar (1.6%), with modest amounts of O_2 and water vapor (Mangold et al., 2016). Trace amounts of other noble gases are present (Ne, Kr, Xe), as well as molecular species such as CO, O_3, NO and H_2O_2, which are produced photochemically from the primary volatiles (Haberle et al., 2017). On Earth, atmospheric CH_4 is mostly produced by biological microbial metabolism and anthropogenic processes, with the remainder being generated by geological processes (Conrad, 2009). On Mars, CH_4 production by atmospheric chemistry is negligible, implying that detections should be considered a signature of either biological or geological activity (e.g., Krasnopolsky et al. (2004)). To date, a seasonally varying background level (e.g., Geminale et al. (2011), Webster et al. (2018)) and short-lived localized plumes (e.g., Giuranna et al. (2019), Mumma et al. (2009), Webster et al. (2015)) have been reported.

The surface of Mars displays a wide variety of geological features, many of which date back to the Noachian period (3.7–4.1 billion years ago) and strongly suggest liquid water once flowed on the surface, potentially creating habitable conditions for microorganisms (e.g., Carr (1996), Grotzinger et al. (2014)). If subsurface aqueous reservoirs exist on Mars today, they may be able to sustain methanogenic organisms. On the other hand, potential sources of methane do not necessarily need to be currently active: formerly produced CH_4 (of biotic or abiotic origin) could be stored in clathrates for later release (Chastain and Chevrier, 2007). Other potential sources of organics are impact metamorphism of already present or meteorically delivered organics and thermogenesis of abiotic or biotic material (Oehler and Etiope, 2017), and water-rock interactions (Etiope et al., 2013; Lyons, 2005). Furthermore, exogenous sources such as in-fall of meteorites (Moores and Schuerger, 2012), and cometary trails (Fries et al., 2016) have been posited. However, the latter process has been questioned as other atmospheric consequences to such a mechanism have not been observed (Crismani et al., 2017a; Roos-Serote et al., 2016).

The photochemical lifetime of CH_4 in the Martian atmosphere is estimated to be around 300 years while the global atmospheric mixing time is on the order of months (Krasnopolsky et al., 2004; Lefèvre and Forget, 2009), implying that CH_4 is expected to be uniformly distributed across the planet once a steady state is reached (Krasnopolsky, 2006; Summers et al., 2002; Viscardy et al., 2016; Waugh et al., 2019). An enhanced level of CH_4 therefore requires an active production or a release mechanism from ancient reservoirs. Without a strong and rapid sink mechanism, CH_4 can potentially be detected long after its initial emission, making it a poor tracker of ongoing activity. However, simulations suggest that if CH_4 is detected shortly (<month) after being emitted from the surface, a highly nonuniform vertical distribution is possible, including the formation of temporary layers (Viscardy et al., 2016). A few weeks after release, the methane is expected to be uniformly mixed. Holmes et al. (2017) showed that to distinguish between sustained and instantaneous surface emissions, at least ten sols of monitoring the emission is necessary. In the same study, it was also found that to distinguish direct surface release from atmospheric destabilization of methane clathrate hydrates, the emission would need to be observed within ten sols of the initial release to avoid it being incorrectly interpreted as a surface emission.

Ethane (C_2H_6) and ethylene (C_2H_4) have shorter photochemical lifetimes (25 years for C_2H_6 (Wong, 2003), and around 1 day for C_2H_4), making them more suitable tracers of recent and current activity if detected. C_2H_6 and C_2H_4 could also aid the degeneracy of potential sources of methane on Mars. From experiments with lightning within volcanic plumes and terrestrial analogs, some geological processes have been shown to release comparable amounts of CH_4 and other hydrocarbons ($CH_4/C_2H_n < 50$), while biological activity generally produces exclusively methane ($CH_4/C_2H_n > 1000$) (Bernard et al., 1977; Segura and Navarro-González, 2005). The presence of ethane and other high-n hydrocarbons in addition to methane is widely accepted to distinguish geological from microbial origin for hydrocarbon gases, but the CH_4/C_2H_n ratio cannot distinguish between ancient biogenic (thermogenic) processes and abiogenic sources related to water-rock reactions (Allen et al., 2006). It must be mentioned that processes could be mixed, and these ratios should not be used as conclusive evidence for excluding either process.

1.1. Previous searches for methane on Mars

Before 2003, all searches for statistically significant methane were negative, or consistent with no observed methane (Krasnopolsky et al., 1997; Lellouch et al., 2000; Maguire, 1977). Since then, detections have been reported by four different groups (Mumma et al., 2003, 2009; Krasnopolsky et al., 2004; Formisano et al., 2004; Webster et al., 2015; Giuranna et al., 2019). Fonti and Marzo (2010) reported a methane detection with the Thermal Emission Spectrometer onboard the Mars Global Surveyor, but during reanalysis the data found the measurements could not unambiguously identify the presence of methane (Fonti et al., 2015). Along with the groups reporting CH_4 detections, four independent searches yielded no methane detections, but upper limits below 15 ppbv (Aoki et al., 2018; Korablev et al., 2019; Krasnopolsky, 2007; Villanueva et al., 2013). Table 1 gives an overview of notable C_2H_6, C_2H_4 and CH_4 searches reported since 2004.

The first reported detection of CH_4 was announced in 2003 (Mumma et al., 2003), and later published in Mumma et al. (2009) after an intensive search in 2003 and 2006 using several ground-based

Table 1
Currently most restrictive upper limits for ethane and ethylene, methane abundances and upper limits below 15 ppbv reported since 2004. Global averages and background values given in brackets.

Species	Abundance	Upper limit	Year of obs.	Reference
Ethane	–	0.2 ppbv[b]	2007	Krasnopolsky (2012)
Ethylene	–	4.1 ppb[a]	2006–2010	Villanueva et al. (2013)
Methane	10 ±3 ppbv[a]	–	1999	Krasnopolsky et al. (2004)
	0–30 ppbv, localized[c] (10 ±5 ppbv, global)[c]	-	2004	Formisano et al. (2004)
	-	14 ppbv[a]	2006	Krasnopolsky (2007)
	5–61 ppbv, localized[d] (14 ±5 ppbv, global)[d]	–	2004–2007	Geminale et al. (2008)
	10–45 ppbv, plumes[a] (3 ppbv, global)[a]	–	2003, 2006	Mumma et al. (2009)
	25–61 ppbv, localized[d] (15 ppbv, global)[d]	–	2004–2009	Geminale et al. (2011)
	3–10 ppbv, localized[b]	8 ppbv[b]	2006, 2009	Krasnopolsky (2012)
	–	6.6 ppbv[a]	2006–2010	Villanueva et al. (2013)
	5.5–9.3 ppbv, plume[b] (0.69 ±0.25 ppbv)[b]	- -	2012–2015	Webster et al. (2015)
	- (0.41 ±0.16 ppbv)[b]	1 ppbv[a] -	2016 2014–2017	Aoki et al. (2018) Webster et al. (2018)
	15.5 ppbv, plume[c]	5 ppbv[c]	2013	Giuranna et al. (2019)
	–	0.05 ppbv[b]	2018	Korablev et al. (2019)

[a] 3-σ uncertainty.
[b] 2-σ uncertainty.
[c] 1-σ uncertainty.
[d] not specified.

observatories. Shortly after the 2003 detection, Krasnopolsky et al. (2004) (utilizing a Fourier Transform Spectrometer at the ground-based Canada-France-Hawaii Telescope) and Formisano et al. (2004) (using the Planetary Fourier Spectrometer (PFS) on the Mars Express (MEX) satellite) reported comparable abundances. In 2007, Krasnopolsky (2007) reported a new upper limit, yet this value was not in conflict with previously published detections. Geminale et al. (2011, 2008) used MEX/PFS to produce temporal and spatial maps of CH_4 by averaging a large number of spectra. Mumma et al. (2009) reported a strong plume of CH_4 in 2003 that subsequently decreased rapidly by 2006. Lefèvre and Forget (2009) pointed out that the destruction mechanism required to explain the observations by Mumma et al. (2009, 2003), and the variations previously seen by Formisano et al. (2004) and Geminale et al. (2008), are unexplained by known atmospheric photochemistry and physical processes on Mars. It was suggested that the detections up to that point should be considered tentative due to several limitations; low spectral resolution for the MEX/PFS detections and the challenge of overlapping telluric and Martian lines for ground-based detections (Encrenaz, 2008). Zahnle et al. (2011) went further, casting doubt on all previous CH_4 detections and raising theoretical objections especially with regards to methane variations. In addition to its challenge to conventional atmospheric chemistry, variable CH_4 on the scale proposed would have major consequences for the Martian atmosphere as a whole; if methane has an unknown chemical sink, it would be by far the biggest term in the atmosphere's redox budget (Zahnle et al., 2011). It has also been implied that analysis of previous obtained MEX/PFS nadir data might be erroneous, following the spot-tracking technique applied by Giuranna et al. (2019). Until 2012, most reported detections agreed on localized plumes (10–45 ppbv), with the possibility of local variations and seasonal changes. Krasnopolsky (2012) searched for CH_4 on two occasions; in 2006 and 2009, where the first dataset shows comparable amounts of methane to previous studies, while the latter dataset found no trace of methane, obtaining an upper limit of 8 ppbv, the lowest upper limit ever reported at that time.

The Mars Science Laboratory Curiosity Rover Tunable Laser Spectrometer (MSL/TLS) has the purported capability of detecting CH_4 at pptv levels (Webster and Mahaffy, 2011). The first report on methane from MSL/TLS obtained the lowest upper limit so far of 1.3 ppbv (Webster et al., 2013), but the results were later revised and detections were reported with an average background level of 0.69 ppbv using the enrichment process, and a plume of 7 ppbv (Webster et al., 2015). This background abundance is lower than model estimates of ultraviolet degradation of infalling interplanetary dust particles (IDP), however Moores and Schuerger (2012) used IDP fluences from Flynn (1996) which were an order of magnitude larger than those recently observed by the Mars Atmosphere and Volatile EvolutioN Mission (Crismani et al., 2017b; Grebowsky et al., 2017).

Villanueva et al. (2013) conducted an exhaustive search for organics in 2006, 2009 and 2010, using the VLT, Keck and IRTF observatories. This search yielded no detections of CH_4 or its oxidation products, and their upper limit of 6.6 ppbv for CH_4 was higher than the averaged abundance (3 ppbv) for 2006 reported in Mumma et al. (2009). However, this non-detection of CH_4 over Valles Marineris by Villanueva et al. (2013) twenty-eight days before the detection by Krasnopolsky (2012) was intriguing, as it may have suggested the presence of large amounts of methane following a rapid release or production event (or issues with the original detection). Aoki et al. (2018) performed sensitive searches for Martian CH_4 by using the Echelon Cross-Echelle Spectrograph onboard the Stratospheric Observatory for Infrared Astronomy, utilizing the high altitude of the instrument which significantly reduced the effects of the terrestrial atmosphere; however, the results showed no unambiguous detections.

Webster et al. (2018) expanded on the results from Webster et al. (2015), adjusting the CH_4 background level once again to 0.41 ppbv, and their enrichment measurements at or near midnight displayed a seasonal behavior. Moores et al. (2019a) suggested that the seasonal variations are consistent with adsorption onto the regolith when combined with diffusion into and out of the regolith, yet point out that the data can only be reconciled when assuming a photochemical lifetime of CH_4 of 400 years in the hypothesis that Gale crater is the only significant emission site on the planet. In addition, Gillen et al. (2020) conducted a statistical analysis on the MSL/TLS dataset and found no evidence for a seasonal CH_4 cycle, stating that the data are too sparse and cover a time span too limited to favor a seasonal period over stochastic variations. The plume reported in Webster et al. (2015) was later reported as confirmed by MEX/PFS (Giuranna et al., 2019) over Gale crater with a slightly higher abundance of 15.5±2.5 ppbv, one sol after the Curiosity detection. There were no detections in any other orbital passages during a two-year period, with the reported upper limit (1-σ) set to 5 ppbv. The results of Webster et al. (2015) have been questioned on the basis of potential rover self-contamination (Zahnle, 2015), while other issues related to the enrichment factor and increases in the methane amount present in the fore-optics were reported in Webster et al. (2018). Two recent papers (Olsen et al., 2020; Trokhimovskiy et al., 2020) identify and quantify trace spectroscopic signatures of O_3 and a magnetic dipole CO_2 band in the 3.3 μm spectral region, near features of the ν_3 band of CH_4. The features do not fully explain the MSL results (Webster et al., 2020), they are relatively weak and do not completely overlap with the methane lines, and therefore they cannot fully account for the reported abundance claims of several ppbv of methane. However, their inclusion is important for improving systematics removal and residual quality.

As summarized above, the detection of methane on Mars has a checkered past, with a strong debate and conflicting claims. New sensitive measurements covering the whole planet are therefore urgently needed. For this, the ExoMars TGO satellite is a highly valuable asset, providing access to tens of ppt sensitivity limits since April 2018 when nominal science operations began. Analysis of the first few months of data yielded no CH_4 detections and set a new upper limit to 0.05 ppbv at 10 km slant altitude, lower than the background levels reported by Curiosity at the surface. More generally, this upper limit strongly questioned all detections reported before, unless a currently unknown rapid sink process is present, particularly in the first few kilometers above the surface. In this paper, we present the first results from a dedicated study of NOMAD data where methane, ethane and ethylene were targeted in solar occultation, and we expand the search for these organics to more than half a Martian Year (MY). This study's primary focus is the effort to detect a methane background level while attempts to discover short-lived plume events were also undertaken.

2. ExoMars TGO/NOMAD instrument and observation

NOMAD consists of three high-resolution spectrometers; SO (Solar Occultation), LNO (Limb, Nadir and Occultation) and UVIS (Ultraviolet and Visible Spectrometer). Technical details on the two infrared channels (SO and LNO) are described in previous works (Vandaele et al., 2018; Neefs et al., 2015; Thomas et al., 2016; Liuzzi et al., 2019; Crismani et al., 2019). TGO's two-hour precessing nearly circular orbit allows for up to 24 occultations per Sol, however the share assigned to NOMAD is typically 12–14 per Sol, with about one occultation every orbit.

The SO channel operates in the wavelength range of 2.2–4.3 μm (2325–4350 cm^{-1}), with a theoretical resolving power ($\lambda/\delta\lambda$) of 20,000 (Vandaele et al., 2018). The channel combines an echelle grating spectrometer with an Acousto-Optical Tunable Filter (AOTF) to select a wavelength region of interest. With a sampling rate of one second, SO provides a raw vertical resolution of ~1 km spanning from near the surface (~5 km) to well above the exobase (~200 km). As the AOTF is able to nearly instantaneously switch between diffraction orders, the SO channel is capable of measuring up to six orders per second.

Solar occultations occur when the instrument is pointed at the solar disk while observing the atmospheric absorption spectrum during ingress and egress. The spectra feature high signal-to-noise ratios due to

the strong solar source. The uppermost part (>200 km) of the occultation corresponds to clear-Sun observations with no atmospheric absorption, which are averaged to obtain a reference spectrum. To compute the transmittance for each measurement, every spectrum below the top of atmosphere is then subsequently divided by the reference spectrum (for details see Liuzzi et al. (2019) and Villanueva et al. (2020)).

As the instrument continuously samples closer to the surface and thereby intersects a larger airmass, the atmospheric absorption increases which decreases the received signal. One of the main limitations to trace gas detection is the presence of clouds and dust aerosols at lower altitudes (Vandaele et al., 2018), which drastically reduces the intensity of light reaching the instrument. Liuzzi et al. (2019) showed that the aerosol load in the Martian atmosphere dramatically impacts the detectability of CH_4 and other trace species in SO geometry, especially at occultation altitudes below 10 km. In SO, the primary sources of stochastic noise in the instrument are the source noise, which depends on the intensity of the source signal (Sun), and the digitization error (14 bits), which is significant when photon counts are low (Neefs et al., 2015). Nevertheless, as long as the observed flux is above a certain threshold (a few percent of the reference spectrum), noise will be dominated by the source, making SO the most sensitive NOMAD channel for the detection of trace species, it also has the key capability of enabling the characterization of their vertical distributions.

3. Dataset and trace gas retrievals

The dataset presented here was acquired by NOMAD from April 2018 to April 2019, corresponding to $L_s = 162.5^\circ$ of MY 34 (Northern hemisphere late summer) to $L_s = 15.0^\circ$ of MY 35 (northern hemisphere early spring). A total of 2819 occultation events containing 243,172 individual spectra were analyzed. To target the molecules of interest (CH_4, C_2H_6, C_2H_4), diffraction orders 133, 134 and 136 were used. Order 133 covers the wavenumber region 2988–3012 cm^{-1} and includes C_2H_6 and C_2H_4 absorption features. Order 134 (3010–3035 cm^{-1}) contains the CH_4 ν_3 Q-branch which peaks at 3018 cm^{-1}, while order 136 (3055–3080 cm^{-1}) contains CH_4 R-branch lines (J = 3 and higher). In absolute terms, the Q-branch is the most intense CH_4 absorption feature, but it is not centered on the detector (diminishing signal at the detector edges owing to reduced blaze throughput) and the presence of nearby solar lines complicates the retrieval. The CH_4 lines in order 136 are more conveniently placed, the line at 3067 cm^{-1} (R4) appearing almost exactly at the center of the detector, however it is partially overlapped by a water line, which occasionally degraded the quality of the retrieval (see spectra in Fig. 8).

The NOMAD detector has 256 rows, where the central 16 are fully illuminated by the Sun. Rows are stacked in groups (i.e., bins) of four prior to any other data modification, and this work utilizes a single such bin. Data calibration and instrument line shape characterization is described in Liuzzi et al. (2019) and remains unmodified for this analysis. The present work used NOMAD level 0.3a data, where the signal acquired by NOMAD is stored in terms of detector counts. From these, data are pre-processed to derive transmittances, using as reference the spectra acquired outside the atmosphere. The process is described in detail in previous works (Aoki et al., 2019; Liuzzi et al., 2020). This preprocessing also takes into account any instrumental temperature-induced frequency shift and produces frequency calibrated residuals. Atmospheric retrievals (excluding CH_4, C_2H_6 and C_2H_4) make use of the Planetary Spectrum Generator (PSG, (Villanueva et al., 2018)), which employs a full atmospheric scattering and radiative transfer package. PSG utilizes up-to-date molecular line lists and implements Optimal Estimation techniques (Rodgers, 2000) modified with an extra regularization parameter (Carissimo et al., 2005; Liuzzi et al., 2016) to perform retrievals, and was used successfully to derive known atmospheric components such as H_2O, HDO and CO_2 (Vandaele et al., 2019; Villanueva et al., 2020). The present work was performed by analyzing residual spectra that were obtained once all known molecular lines along with stellar, water ice and broadband dust features were fitted with PSG and filtered out, leaving only the eventual signal from minor trace species in the residuals.

To limit the effects of the relevant noise sources in the SO channel, all measurements whose continuum transmittance was below 5% were excluded from further analysis. Dust storm season on Mars occurs every year from $L_s = 180^\circ$-360°, when the planet is closest to the Sun and overall surface and atmospheric temperatures are warmest (Smith, 2008). However, MY 34 saw a higher dust aerosol load than normal as for the first time since 2007, Mars was obscured by a Global Dust Storm (GDS). The GDS caused elevated dust aerosol loading across the entire planet during $L_s = 180^\circ$-250°, and from $L_s = 315^\circ$-345° a strong regional dust storm occurred (Smith, 2019). Due to the dust storm season on Mars, the most sensitive upper limits were obtained using observations that were taken right after the beginning of science operations, and also towards the end of this dataset.

In an effort to discover hydrocarbon signals, we compared measured atmospheric residual spectra with synthetic trace gas spectra generated using PSG. The occurrence of remnant broad continuum features in the residuals is still possible due to instrument variations not fully accounted for (see Liuzzi et al. (2019) for further details). Therefore, after retrieval of all expected species, a 3-spectrum moving mean was performed on the residuals to increase sensitivity, with a resulting vertical resolution of typically 2 km. For diffraction order 136 (~ 12% of the data), where the methane lines are sharp and narrow, a 10-pixel smoothed residual spectrum was removed from the residual to mitigate some of the broader non-molecular residual variability in the spectral continuum. This step is omitted for the other orders where the absorption features are broader. A Levenberg-Marquardt least-squares method was used to fit the atmospheric residuals to a synthetic spectrum produced with PSG, with prescribed column abundances for the target species. The first and last ten pixels of each spectrum were excluded from the fitting procedure due to diminishing signal at the detector edges owing to reduced blaze throughput (see Liuzzi et al. (2019) for further discussion). The trace gas retrieval used reduced chi-square analysis to determine retrieval parameters by minimization.

This algorithm produced two outputs for each retrieval: the covariance matrix of the fitted parameters whose diagonal values correspond to the square of the uncertainty of every parameter, and the optimal value for the scaling parameter, which corresponds to the relative amplitude of the synthetic model that best fits the data. The upper limit is defined as the retrieved uncertainty of the trace gas line-of-sight density divided by the total atmospheric line-of-sight density. The attempted retrieved abundance is defined as the optimal scaling parameter multiplied by the ratio of trace gas abundance in the synthetic model to CO_2 line-of-sight density. A statistical sensitivity study was then carried out on these two values.

Fig. 1 shows the retrieved abundance mixing ratio (blue) and 2-σ upper limit (black) (both in ppbv) by altitude for one occultation. At higher altitudes, the retrieved upper limits are dominated by the line-of-sight airmass, while at a certain point increasing aerosol opacity reduces the received signal such that low photon counts introduce noise from instrument systematics. The spectrum with the smallest upper limit is found where limiting factor is minimum, corresponding to a transition from one factor being dominant to the other. The altitude at which this transition occurs is dependent on the atmospheric aerosol opacity. The spectrum nearest this noise transition is henceforth referred to as the principal point.

To condense the dataset into a collection of the most relevant datapoints, a spectrum at or close in altitude to the principal point was selected for every occultation for each targeted trace gas. The retrieved abundances (in ppbv) for the selected spectra corresponding to these principal points were divided by their 1-σ uncertainty values, yielding the uncertainty normalized abundance (UNA). Assuming the estimated input noise in the retrieval is independent of geometric (latitude-

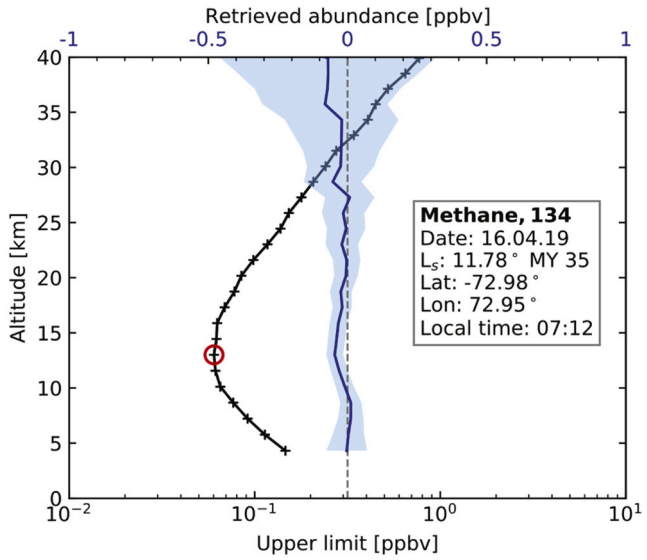

Fig. 1. An example of retrieved abundance (blue) and the corresponding derived upper limits (black) for all spectra in a single occultation as a function of altitude, targeting CH_4 in order 134. The shaded blue area indicates the ± 1-σ confidence interval. The red circle indicates the location of the principal point, the residual with smallest upper limit. (For interpretation of the references to color in this figure legend, the reader is referred to the web version of this article.)

longitude), seasonal (Ls), and orbital (e.g., heliocentric distance) factors, the histogram containing all UNA values should behave as a Gaussian distribution with a standard deviation of one centered on the average UNA. If there is no detectable trace gas present and only random Gaussian noise is measured, given a large sample number, the histogram should be centered on zero. Fig. 2 displays the histograms for each diffraction order, where the top row includes every spectrum from all occultations, and the bottom row includes only the principal point spectra, selected as demonstrated in Fig. 1.

A standard deviation of less than one, as seen for the ethylene histograms, indicates that the true noise is larger than what was estimated for the retrieval. Order 134 was measured with significantly higher cadence than the other diffraction orders which aided in the statistical validity of the histogram results, where for Poisson-derived noise, the uncertainty on the sample mean is reduced with the square root of the sample size. In Section 4, only the principal point spectra from each occultation is evaluated. These measurements represent the most sensitive observations in the dataset and still number in the thousands for CH_4 and hundreds for C_2H_6 and C_2H_4, an analysis of these observations are therefore statistically significant.

4. Results

This dataset samples the dawn and dusk terminators, latitudes from 85°S to 85°N, all longitudes, and altitudes from 5 to 100 km. All altitude values used in this work are in terms of true distance to the surface. Retrievals were organized by season and upper limit, where those dedicated to CH_4 are subsequently arranged by longitude and latitude, as well as latitude and altitude to explore various morphology aspects. The search for methane on Mars is twofold, partly exploring the existence of a global, albeit low, seasonally varying background level (Formisano et al., 2004; Geminale et al., 2008; Webster et al., 2018), and partly focusing on the appearances of strong and localized short-term plumes (Giuranna et al., 2019; Mumma et al., 2009; Webster et al., 2015). As the detection of short-lived events relies heavily on observing the right place at the right time, this work prioritized the search for a CH_4 background level.

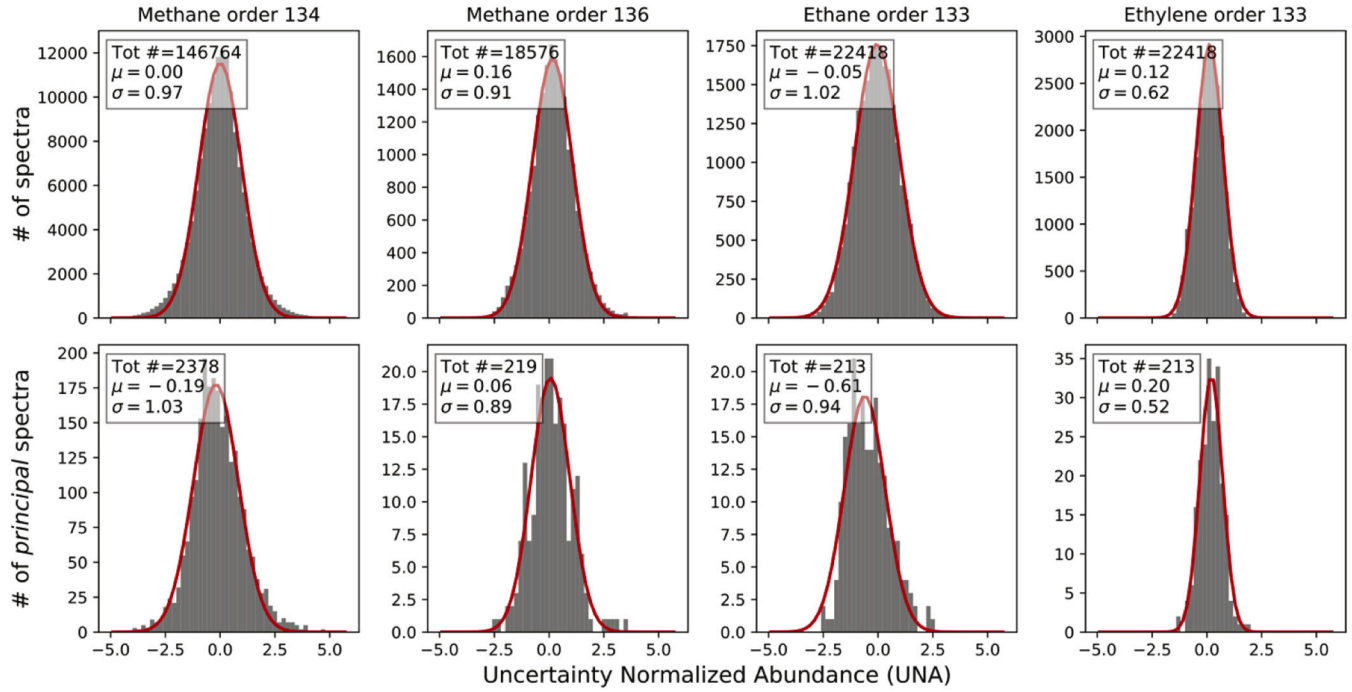

Fig. 2. Histograms visualizing the distribution of retrieved abundances normalized by the 1-σ uncertainty value (UNA). The top row includes every data point from all occultations, while the bottom row includes only the principal point from each occultation. The two first columns show methane in orders 134 and 136, while the third and fourth columns show ethane and ethylene in order 133. The red curves show the Gaussian that best fits the dataset; the mean value (μ), standard deviation (σ) and total number of spectra are shown for each dataset. (For interpretation of the references to color in this figure legend, the reader is referred to the web version of this article.)

4.1. Ethane & ethylene retrievals

Ethane and ethylene were targeted in 213 occultations (28,470 atmospheric spectra) using order 133. The principal point (spectrum with the smallest retrieved upper limit in each occultation) was selected by the approach described in Section 3 and visualized in Fig. 1. C_2H_6 and C_2H_4 upper limits are plotted in Fig. 3 where they are shown as a function of season, the color scale indicates altitude.

The retrieved upper limits demonstrably degraded as dust storm season and the GDS commenced at $L_s = 180°$ with higher dust aerosol opacity reducing the received signal along the line of sight. Even as the GDS dissipated around $L_s = 250°$, the upper limits remained high until some time after the dust storm season ended at $L_s = 360°$. The enhanced aerosol content in the lower atmosphere raised the altitude of the principal points, resulting in the smallest upper limits for ethane and ethylene being obtained around $L_s = 12°$.

The smallest upper limits are useful when searching for a low, global background level of a trace gas, and such a spectrum is shown in Fig. 4, panel A. As ethane and ethylene have relatively short photochemical lifetimes in the Martian atmosphere, a constantly present background level requires continuous replenishment. Therefore, in the attempt to discover short-lived plumes, the most suitable strategy is to investigate spectra with high UNA, falling on the right wing of the histograms in Fig. 2. Residuals for the measurement with highest UNA below 30 km for each gas are shown in Fig. 4B and C. Known solar and Martian atmospheric absorption lines were removed, leaving featureless residual spectra. The lowest upper limit for ethane was determined to be 0.11 ppbv, and 0.7 ppbv for ethylene, both significantly lower than previous upper limits (see Table 1). The upper limits obtained for the high UNA spectra are 0.4 ppbv (UNA =2.23) and 3.6 ppbv (UNA =1.25) for ethane and ethylene respectively. The high UNA is the result of a combination of relatively high retrieved abundance and a comparably low noise level.

4.2. Methane retrievals

The search for CH_4 is one of the primary objectives of ExoMars TGO and NOMAD (Vandaele et al., 2015). For this work, order 134 is used to target the CH_4 Q-branch, while order 136 contains the R-branch lines. The dataset includes 2385 occultations where order 134 was measured, along with 221 occultations for order 136, totaling more than 210,000 spectra able to target methane. For each occultation, a spectrum near in altitude to the principal point was selected and the upper limits are mapped onto the Martian surface in Fig. 5.

Methane measurements span all longitudes and latitudes, however datapoints at low latitudes have larger upper limits than those found at higher latitudes. This correlation is attributed to the tendency of lower latitudes typically having a higher dust aerosol load than high-latitude regions, which raised the atmospheric opacity near equatorial latitudes and thus prevented sensitive measurements. The low number of measurements near the equator (± 20°) is related to the orbital geometry of solar occultation measurements, representing 10% of the total number of measurements. Low latitude datapoints subsequent to April 2019 are expected to have higher sensitivity as Mars enters the aphelion season, during which dust activity is greatly reduced (Smith, 2008).

Due to the orbit of TGO, latitudinal changes are convolved with seasonal variation, since the orbit precesses on a timescale similar to expected seasonal changes. The best upper limit for each occultation is presented in Fig. 6 as a function of Martian season L_s. The principal points with the lowest upper limits were obtained at the beginning and towards the end of TGO's first year of observations. They tend to be taken at lower altitudes where the spacecraft is observing through a large airmass, which increases the relative depth of the lines.

Methane upper limits have been explored spatially in Fig. 5, and as a function of time (season) in Fig. 6. In order to explore the altitude distribution of the upper limits, Fig. 7 shows the principal points for CH_4 for all longitudes from all occultations as a function of latitude and altitude. Fig. 7 demonstrates that even in the presence of two dust storms, a large number of sensitive measurements probed altitudes below the lowest

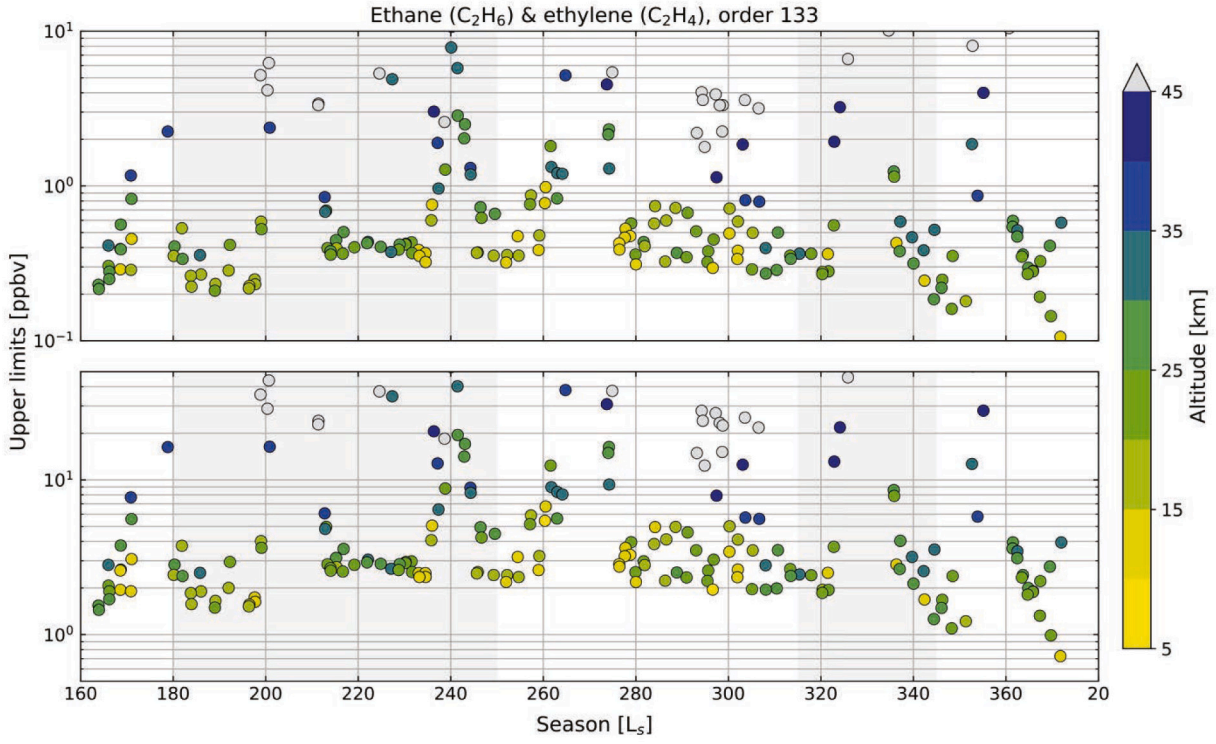

Fig. 3. The principal point (smallest upper limit) for each occultation below 10 ppbv, for ethane (top panel) and ethylene (bottom panel) in order 133, shown as a function of season, where the colors indicate altitude. Shaded gray areas indicate times of enhanced aerosol opacity.

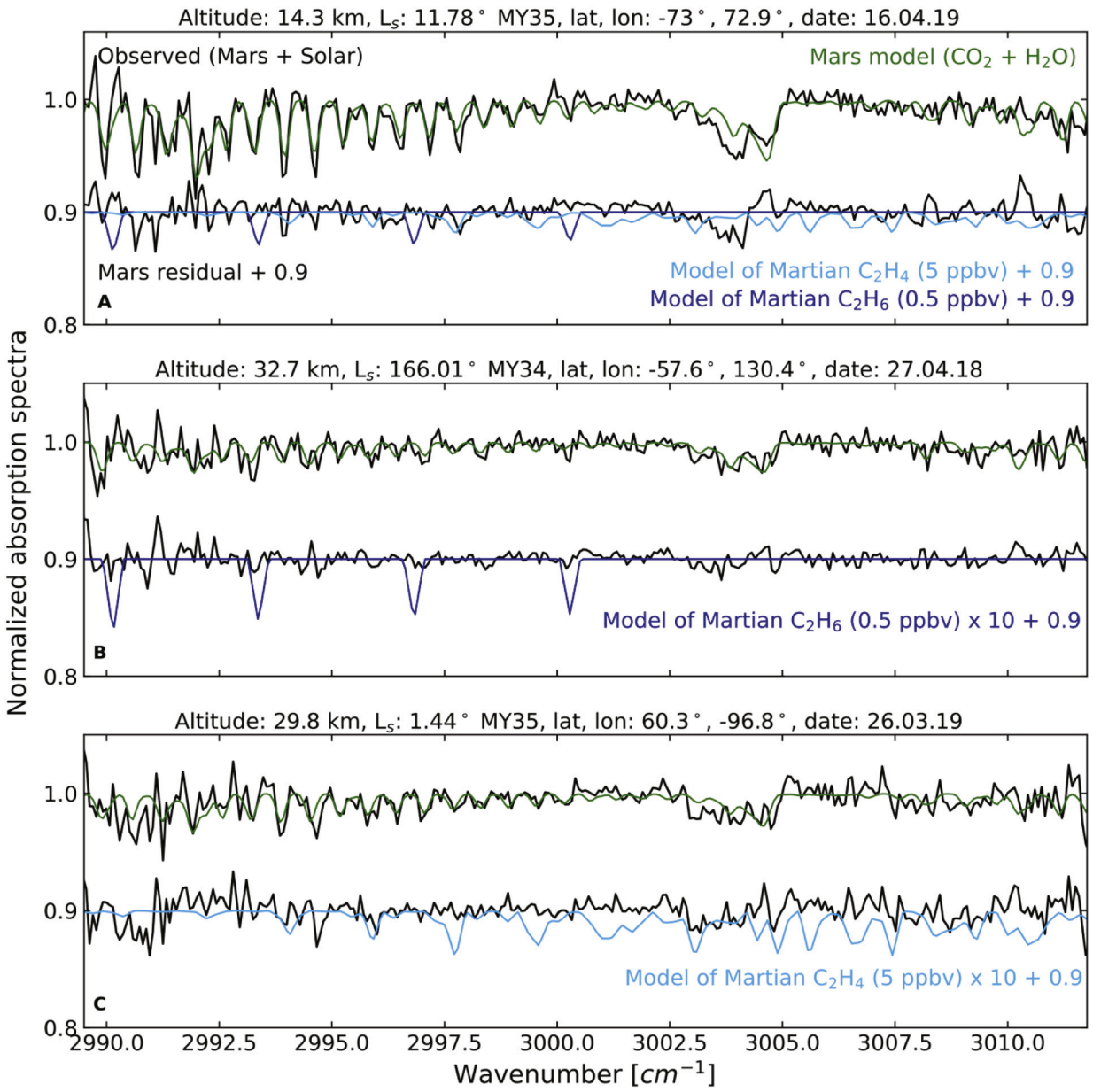

Fig. 4. Sensitive search for ethane and ethylene on Mars. A) targeting spectra with smallest upper limits. B) & C) targeting spectra with high UNA. Observed spectra in black, PSG model fit to the Martian atmosphere in green, synthetic spectra of trace species in hues of blue. All spectra are scaled with a factor of 10 to optimize visibility, in addition to scaling factors mentioned in the figure itself. (For interpretation of the references to color in this figure legend, the reader is referred to the web version of this article.)

two scale heights (<20 km). Grain-gas interactions in the lower one to two scale heights such as oxidization (Atreya et al., 2006) and reactions with eroded quartz (Knak Jensen et al., 2014) have been proposed as potential, and the latter is currently considered one of the most plausible candidates for a CH_4 loss process (Yung et al., 2018). However, as NOMAD is obtaining high-sensitivity measurements down into the lowest scale height of the Martian atmosphere, this hypothesis may require additional investigation to be considered feasible in the Martian atmosphere.

To establish whether a persistent background level of methane can be detected by NOMAD, the principal points would need to be collected and analyzed as a whole, whereas selecting the measurements with the highest UNA is a more appropriate approach when searching for short-lived events such as potential plumes. The entire principal point dataset contains five measurements with UNA at or above 5-σ. To investigate such a high σ "detection", Fig. 8C is constructed to highlight the residual of a principal point spectrum located at the positive wing of the histograms in Fig. 2. The spectrum in Fig. 8C has an UNA of 5.1, suggesting a 5-σ detection of 0.66 ppbv. However, upon inspection of the residual it becomes evident that there is no clear detection of CH_4, and instead this 5-σ result is the consequence of residual systematics related to digitization error. Generally, the occurrence of high- σ detections is an expected effect when measuring Poisson noise on repeated observations. Table 2 presents a summary of the upper limits and the geophysical details for each spectrum shown in Fig. 8.

The spectrum with lowest upper limit obtained from this entire study is shown in Fig. 8A, with a retrieved upper limit of 0.061 ppbv. The spectrum closest to the surface (Fig. 8B) has a retrieved upper limit of 0.30 ppbv, and the spectrum with an UNA of 5 (Fig. 8C) has an upper limit of 0.66 ppbv. The most sensitive measurement and the one with highest UNA were achieved with order 134, while the spectrum lowest in altitude was attained with order 136. The residual spectra displayed

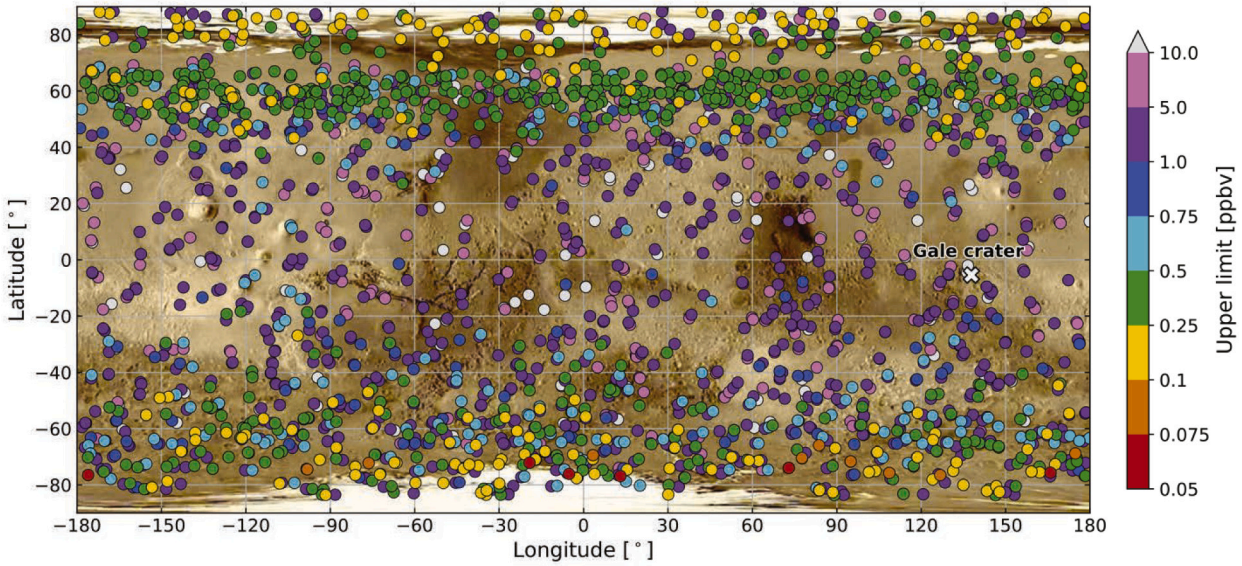

Fig. 5. All principal points for CH_4 in orders 134 and 136. Visualized on a latitude-longitude map with Gale crater (position of Curiosity rover) marked by a white cross. colors indicate the derived upper limits for abundance values within a 95% confidence interval (2-σ). The indicators are sorted, with the smallest upper limits shown on top.

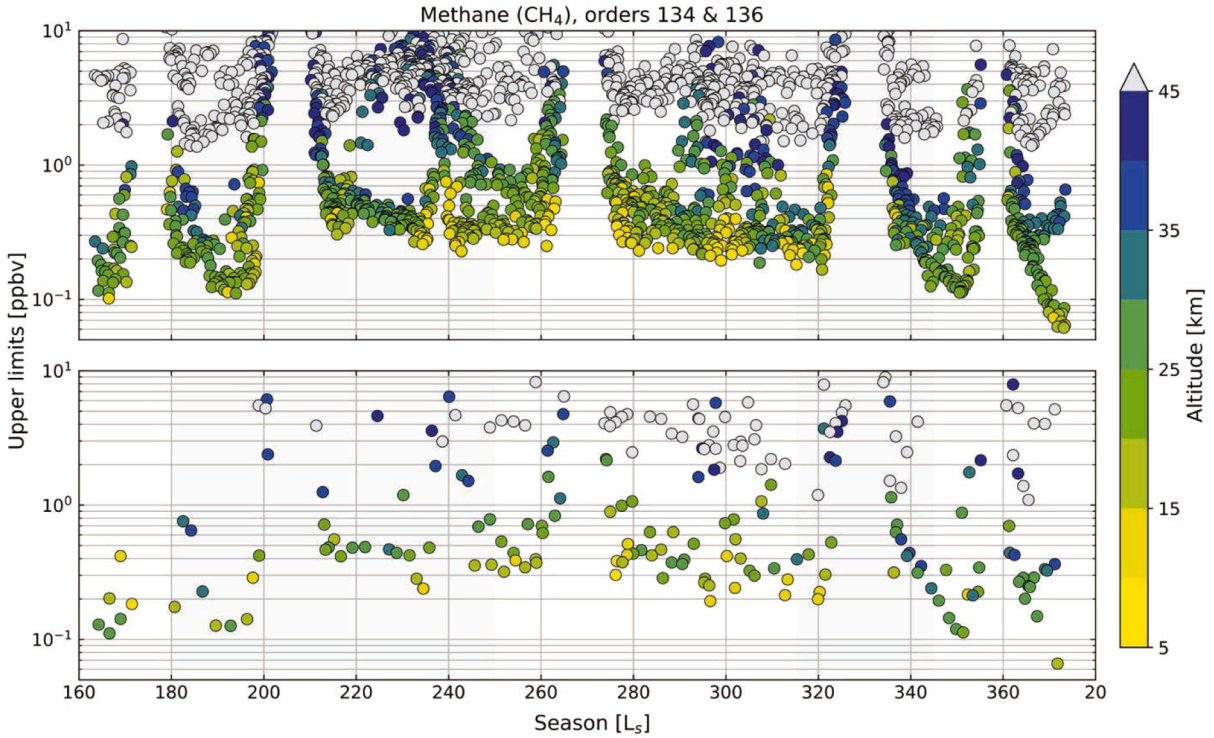

Fig. 6. The principal points for CH_4 from each occultation, for order 134 (top row) and 136 (bottom row) plotted as a function of season, where the colors indicate altitude. Methane upper limits increased significantly while the planet was engulfed by the GDS (L_s = 195°-280°). Shaded gray areas indicate times of enhanced aerosol opacity.

in Fig. 8 are without significant features and considering the strong signal a plume-like event is likely to cause, NOMAD would be able to detect it if present in the current data set or in the future.

5. Discussion

Methane detections reported by several groups over the past fifteen years suggest localized regions of sporadic gaseous release from unknown sources and with an unknown fast and efficient destruction mechanism. Previous ground-based and Mars Express orbital detections reported column densities for the whole atmosphere, apart from Curiosity which takes measurements at the surface within Gale crater. The data presented here are solar occultation measurements, sampling the atmosphere at specific slant heights, obtaining a typical vertical resolution of 2 km, with the lowest measured principal point close to 6 km above the Martian surface. CH_4 background levels have been reported to

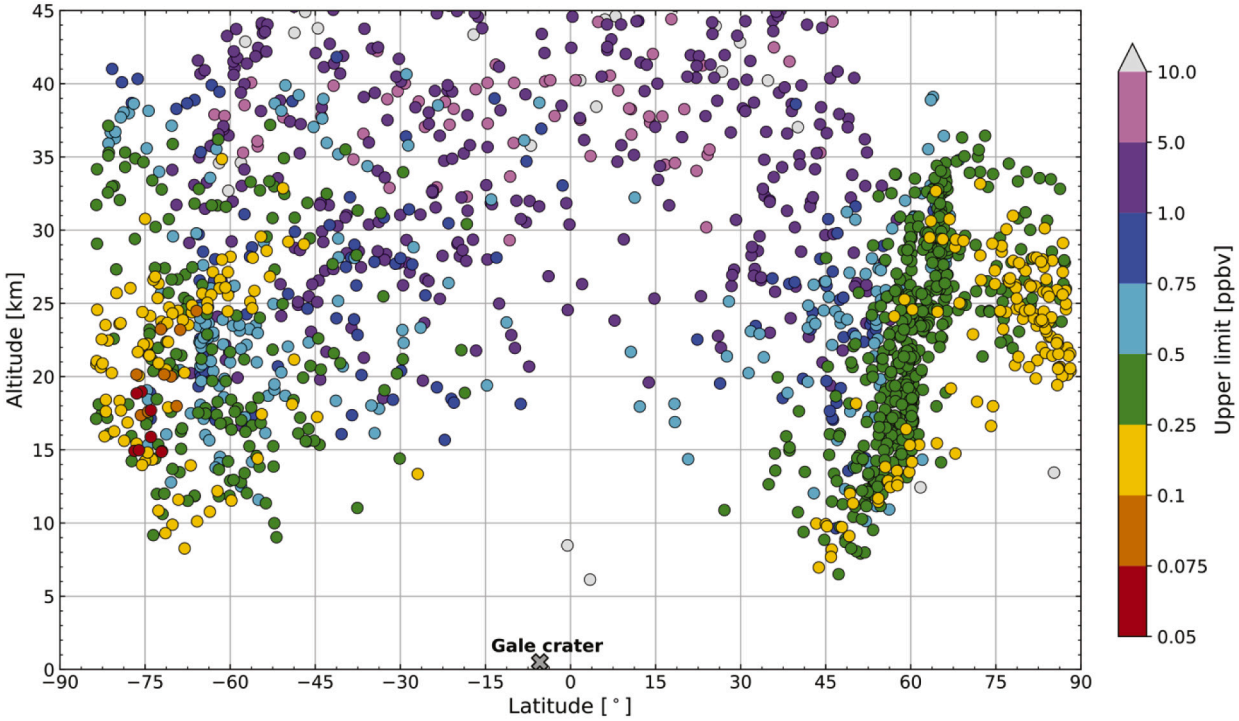

Fig. 7. Principal CH_4 points from all occultations for diffraction orders 134 and 136 for all longitudes, as a function of altitude and latitude. The colors indicate upper limits. Green, yellow, orange and red indicators are values at or below the average background level observed by Webster et al. (2018). The gray cross indicates position of the Curiosity rover in Gale crater. (For interpretation of the references to color in this figure legend, the reader is referred to the web version of this article.)

vary, perhaps on a seasonal basis, and a large outgassing event was reportedly detected by two independent teams (Giuranna et al., 2019; Webster et al., 2015). From our current understanding of the Martian atmosphere, any seasonal, periodic or even sporadic release of CH_4 will lead to its accumulation over time, increasing the chances for its detection (Lefèvre, 2019). Moreover, any methane released from the surface would in the matter of days be transported to altitudes where it could be detected by TGO/NOMAD (Viscardy et al., 2016). Geminale et al. (2011) reported a strong increase in CH_4 up to 45 ppbv over the northern polar cap during northern summer, along with higher abundances in general during northern spring compared to fall and winter, related to a possible methane source under the polar cap. However, Lefèvre and Forget (2009) showed that in the event of a methane release, the gas would quickly be globally distributed, and during northern winter a large enrichment in methane mixing ratio resulting from the condensation of CO_2 gas at high latitudes would occur. TGO/NOMAD sampled high latitudes during late northern summer as well as northern winter and found no detections during either season.

All reported CH_4 detections, apart from the Curiosity measurements and the Giuranna et al. (2019) findings from June 2013, are at least eleven years old. The most recently reported background level from MSL/TLS claimed 0.319 ppbv on May 17th, 2017 (Webster et al., 2018), less than an Earth year prior to TGO's first measurements which revealed an upper limit three times lower. The largest plume ever recorded, and the most recent MSL methane data, was mentioned in Moores et al. (2019b), with a value of 19±3 ppbv on June 20th 2019, while NOMAD data acquired only two months earlier yielded some of the lowest upper limits obtained with the instrument. It is important to note that Curiosity/MSL samples the atmosphere at the surface, while no TGO/NOMAD measurements below 6 km have been analyzed in this work. To reconcile these results, one would need to include an atmospheric process where CH_4 is rapidly removed from the lower atmosphere. Any such strong destruction mechanism should not affect known and confirmed knowledge about the Martian atmosphere and its chemical composition.

Moores et al. (2019a) explored the possibility of a diurnal cycle to reconcile MSL and TGO observations by modeling a surface microseepage flux and diffusivity in the Martian nighttime atmosphere. They propose an inhibition of atmospheric mixing near the Gale crater surface overnight, enabling methane being emitted to accumulate. Another reconciliating process could be by direct electron dissociation during dust storms (Farrell et al., 2006), but highly sensitive NOMAD measurements right before the dust storm, when there could have been methane present, show extremely low upper limits (Fig. 6). Other grain-gas interactions could take place near the surface; oxidant-covered soil particles could rapidly oxidize CH_4 before it can be transported to other regions (Atreya et al., 2006), or methane could be sequestered by eroded quartz grains (Knak Jensen et al., 2014). The latter mechanism is considered quite plausible (Yung et al., 2018), although its efficiency has been questioned (Lefèvre, 2019) and the laboratory work did not include any other atmospheric species in their experiment apart from CO_2, thus neglecting the impact on and by other species (Knak Jensen et al., 2014). It should be noted that NOMAD's most sensitive searches are between 6 and 15 km in altitude (Fig. 7).

Localized surface sinks have been explored by Lefèvre and Forget (2009), who found that for their model to match observations, methane would have a lifetime of an hour at the atmosphere-regolith interface. Any additional mechanism dominating the removal of CH_4, has to be more efficient than currently understood photochemistry by a factor of $\geq$100 and would need to destroy or sequester CH_4 without violating the chemistry of active species such as O_3, CO or H_2O_2, which are reproduced by existing models without unknown processes. If methane is indeed released from sub-surface reservoirs into the Martian atmosphere, the question of a strong destruction mechanism remains unresolved. To reconcile results from MSL and TGO, future work would benefit from focusing on understanding near-surface destruction mechanisms.

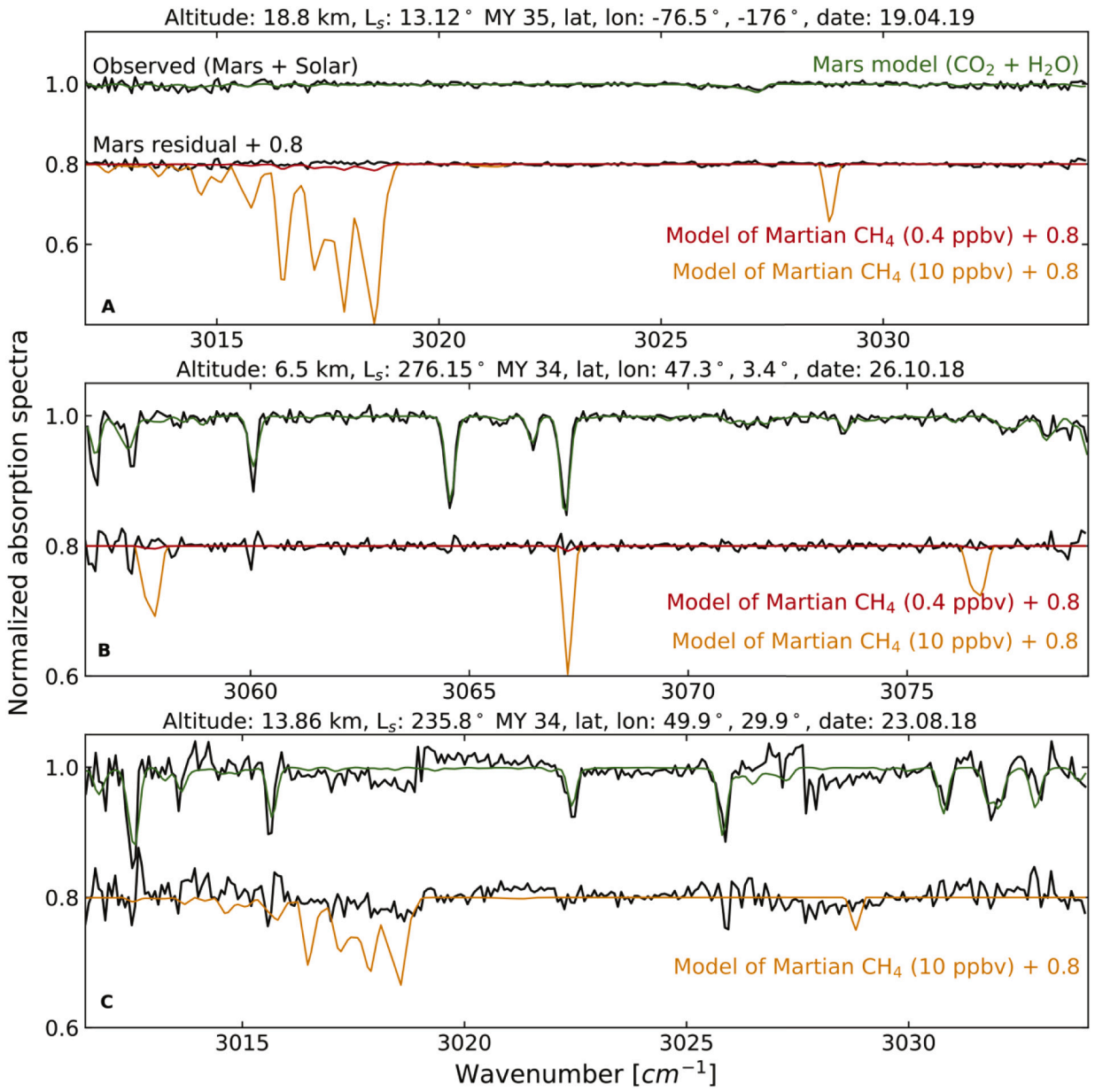

Fig. 8. Search for methane on Mars by three methods; A) spectrum with lowest retrieved upper limit, B) spectrum with principal point closest to surface, C) spectrum with high UNA in search of plume. Observed spectra are shown in black, PSG model fit to the main gases (H_2O and CO_2) in green and synthetic CH_4 spectra in red and orange. The red spectrum of 0.4 ppbv abundance is used to visualize previously observed background level and the orange spectrum of 10 ppbv abundance simulates a sporadic plume event. All spectra in panel A are scaled by a factor of 10, and all spectra in panel C are scaled by a factor of 2. (For interpretation of the references to color in this figure legend, the reader is referred to the web version of this article.)

Table 2
The lowest obtained upper limits for the three target species. Lowest methane upper limits achieved with order 134. Ethane and ethylene were both retrieved from order 133.

Trace gas	Upper limit	Altitude	Lat, Lon	Ls	Date
Methane	0.061 ppbv	18.8 km	−76.5°, −176°	13.12°	19.04.19
Ethane	0.1 ppbv	14.3 km	−73°, 72.9°	11.78°	16.04.19
Ethylene	0.7 ppbv	14.3 km	−73°, 72.9°	11.78°	16.04.19

6. Conclusion

In this study, methane, ethane and ethylene retrieval attempts were conducted on atmospheric residual spectra (see Table 2). In contrast with previous total atmospheric column measurements (i.e., ground-based, Mars-Express) and surface measurements (i.e., MSL), TGO is able to probe the atmosphere with high sensitivities above 6 km and with fine vertical resolution (~2 km as presented here). The uncertainty normalized abundances follow a Gaussian distribution and their mean values are at or close to zero, suggesting there are no detections of organics in the dataset, thus the upper limit is defined as the 2-σ uncertainty value for each retrieval. The upper limits presented in this work, and the detection limit of NOMAD, are at this moment dominated by systematics. Future efforts should focus on improvements in NOMAD characterization stability across the occultation, and refining the modeling of known molecular lines with an improved instrument lineshape. Furthermore, expansion of the dataset beyond the Martian dust season will yield more sensitive datapoints at low latitudes and altitudes.

The upper limits for ethane and ethylene provide significant

improvements compared to previous studies, lowering these by a factor of 2–5. However, the values are at least a factor of six higher than the methane upper limit, and thus cannot contribute to narrowing down possible origins for the hydrocarbons, if they were found to be present.

Methane detection attempts were made at all latitudes and longitudes, at slant altitudes from 5 to 100 km, and sampled at dawn and dusk local times. No background level of CH_4 was detected down to 0.06 ppbv, and no intense short-lived plume events were observed. Our methane upper limit is consistent with the average value reported by Korablev et al. (2019). If methane is being released into the atmosphere, this process would need to be sporadic and undetected in this year of observations. Moreover, whether the presumed release is global or local, an unknown destruction mechanism would also need to efficiently remove the methane before vertical mixing can bring it above 6 km (i.e., within a few days (Viscardy et al., 2016)), or else the release is local and concentrated enough that mixing depletes the concentrations well below any potential detection threshold at those altitudes accessible by TGO/NOMAD.

Declaration of Competing Interest

The authors declare that they have no known competing financial interests or personal relationships that could have appeared to influence the work reported in this paper.

Acknowledgements

The NOMAD experiment is led by the Royal Belgian Institute for Space Aeronomy (IASB-BIRA), assisted by Co-PI teams from Spain (IAA-CSIC), Italy (INAF-IAPS), and the United Kingdom (Open University). This project acknowledges funding by the Belgian Science Policy Office (BELSPO), with the financial and contractual coordination by the ESA Prodex Office (PEA 4000103401, 4000121493), by Spanish Ministry of Science and Innovation (MCIU) and by European funds under grants PGC2018-101836-B-I00 and ESP2017-87143-R (MINECO/FEDER), as well as by UK Space Agency through grants ST/V002295/1, ST/V005332/1 and ST/S00145X/1 and Italian Space Agency through grant 2018-2-HH.0. This work was supported by the Belgian Fonds de la Recherche Scientifique – FNRS under grant number 30442502 (ET_HOME). The IAA/CSIC team acknowledges financial support from the State Agency for Research of the Spanish MCIU through the 'Center of Excellence Severo Ochoa' award for the Instituto de Astrofísica de Andalucía (SEV-2017-0709). Canadian investigators were supported by the Canadian Space Agency. This work was supported by NASA's Mars Program Office under WBS 604796, "Participation in the TGO/NOMAD Investigation of Trace Gases on Mars". MC is supported by the NASA Postdoctoral Program at the NASA Goddard Space Flight Center, administered by Universities Space Research Association (USRA) under contract with NASA. S. A. is "Chargé de Recherches" at the F.R.S.-FNRS. We would also like to thank Dr. Sara Faggi for valuable advice, expertise and continuous support during this study.

References

Allen, M., Sherwood Lollar, B., Runnegar, B., Oehler, D.Z., Lyons, J.R., et al., 2006. Is Mars alive? EOS Trans. Am. Geophys. Union 87, 433. https://doi.org/10.1029/2006EO410001.

Aoki, S., Richter, M.J., DeWitt, C., Boogert, A., Encrenaz, T., et al., 2018. Stringent upper limit of CH4 on Mars based on SOFIA/EXES observations. Astron. Astrophys. 610, A78. https://doi.org/10.1051/0004-6361/201730903.

Aoki, S., Vandaele, A.C., Daerden, F., Villanueva, G.L., Liuzzi, G., et al., 2019. Water vapor vertical profiles on Mars in dust storms observed by TGO/NOMAD. J. Geophys. Res. Planets 124, 3482–3497. https://doi.org/10.1029/2019JE006109.

Atreya, S.K., Gu, Z.G., 1995. Photochemistry and stability of the atmosphere of Mars. Adv. Space Res. 16, 57–68. https://doi.org/10.1016/0273-1177(95)00250-I.

Atreya, S.K., Wong, A.-S., Renno, N.O., Farrell, W.M., Delory, G.T., et al., 2006. Oxidant enhancement in Martian dust devils and storms: implications for life and habitability. Astrobiology 6, 439–450. https://doi.org/10.1089/ast.2006.6.439.

Bernard, B., Brooks, J.M., Sackett, W.M., 1977. A geochemical model for characterization of hydrocarbon gas sources in marine sediments, in: offshore technology conference. In: Presented at the Offshore Technology Conference, Offshore Technology Conference, Houston, Texas. https://doi.org/10.4043/2934-MS.

Carissimo, A., De Feis, I., Serio, C., 2005. The physical retrieval methodology for IASI: the δ-IASI code. Environ. Model. Softw. 20, 1111–1126. https://doi.org/10.1016/j.envsoft.2004.07.003.

Carr, M.H., 1996. Water erosion on Mars and its biologic implications. Endeavour 20, 56–60. https://doi.org/10.1016/0160-9327(96)10013-2.

Chastain, B.K., Chevrier, V., 2007. Methane clathrate hydrates as a potential source for martian atmospheric methane. Planet. Space Sci. 55, 1246–1256. https://doi.org/10.1016/j.pss.2007.02.003.

Conrad, R., 2009. The global methane cycle: recent advances in understanding the microbial processes involved: global methane cycle. Environ. Microbiol. Rep. 1, 285–292. https://doi.org/10.1111/j.1758-2229.2009.00038.x.

Crismani, M.M.J., Schneider, N.M., Plane, J.M.C., 2017a. Comment on "A cometary origin for atmospheric martian methane" by Fries et al., 2016. Geochem. Perspect. Lett. https://doi.org/10.7185/geochemlet.1715.

Crismani, M.M.J., Schneider, N.M., Plane, J.M.C., Evans, J.S., Jain, S.K., et al., 2017b. Detection of a persistent meteoric metal layer in the Martian atmosphere. Nat. Geosci. 10, 401–404. https://doi.org/10.1038/ngeo2958.

Crismani, M.M.J., Villanueva, G.L., Liuzzi, G., Mumma, M.J., Smith, M.D., Vandaele, A.C, Aoki, S., Thomas, I.R., Daerden, F., Lopez-Valverde, M.A., Ristic, B., Patel, M.R., Bellucci, G., Lopez-Moreno, J-J., et al., NOMAD Science Team, 2019. Maps of Martian Atmospheric H2O with Trace GasOrbiter's NOMAD/LNO. 13. In: EPSC-DPS Joint Meeting.

Encrenaz, T., 2008. Search for methane on Mars: observations, interpretation and future work. Adv. Space Res. 42, 1–5. https://doi.org/10.1016/j.asr.2007.01.069.

Etiope, G., Ehlmann, B.L., Schoell, M., 2013. Low temperature production and exhalation of methane from serpentinized rocks on earth: a potential analog for methane production on Mars. Icarus 224, 276–285. https://doi.org/10.1016/j.icarus.2012.05.009.

Farrell, W.M., Delory, G.T., Atreya, S.K., 2006. Martian dust storms as a possible sink of atmospheric methane. Geophys. Res. Lett. 33, L21203 https://doi.org/10.1029/2006GL027210.

Flynn, G.J., 1996. The delivery of organic matter from asteroids and comets to the early surface of Mars. In: Rickman, H., Valtonen, M.J. (Eds.), Worlds in Interaction: Small Bodies and Planets of the Solar System. Springer Netherlands, Dordrecht, pp. 469–474. https://doi.org/10.1007/978-94-009-0209-1_58.

Fonti, S., Marzo, G.A., 2010. Mapping the methane on Mars. Astron. Astrophys. 512, A51. https://doi.org/10.1051/0004-6361/200913178.

Fonti, S., Mancarella, F., Liuzzi, G., Roush, T.L., Chizek Frouard, M., et al., 2015. Revisiting the identification of methane on Mars using TES data. Astron. Astrophys. 581, A136. https://doi.org/10.1051/0004-6361/201526235.

Formisano, V., Atreya, S., Encrenaz, T., Ignatiev, N., Giuranna, M., 2004. Detection of methane in the atmosphere of Mars. Science 306, 1758–1761. https://doi.org/10.1126/science.1101732.

Fries, M., Christou, A., Archer, D., Conrad, P., Cooke, W., et al., 2016. A cometary origin for martian atmospheric methane. Geochem. Perspect. Lett. 2, 10–23. https://doi.org/10.7185/geochemlet.1602.

Geminale, A., Formisano, V., Giuranna, M., 2008. Methane in Martian atmosphere: average spatial, diurnal, and seasonal behaviour. Planet. Space Sci. 56, 1194–1203. https://doi.org/10.1016/j.pss.2008.03.004.

Geminale, A., Formisano, V., Sindoni, G., 2011. Mapping methane in Martian atmosphere with PFS-MEX data. Planet. Space Sci. 59, 137–148. https://doi.org/10.1016/j.pss.2010.07.011.

Gillen, E., Rimmer, P.B., Catling, D.C., 2020. Statistical analysis of curiosity data shows no evidence for a strong seasonal cycle of martian methane. Icarus 336, 113407. https://doi.org/10.1016/j.icarus.2019.113407.

Giuranna, M., Viscardy, S., Daerden, F., Neary, L., Etiope, G., et al., 2019. Independent confirmation of a methane spike on Mars and a source region east of Gale crater. Nat. Geosci. 12, 326–332. https://doi.org/10.1038/s41561-019-0331-9.

Grebowsky, J.M., Benna, M., Plane, J.M.C., Collinson, G.A., Mahaffy, P.R., et al., 2017. Unique, non-earthlike, meteoritic ion behavior in upper atmosphere of Mars: Mars metal ions. Geophys. Res. Lett. 44, 3066–3072. https://doi.org/10.1002/2017GL072635.

Grotzinger, J.P., Sumner, D.Y., Kah, L.C., Stack, K., Gupta, S., et al., 2014. A habitable Fluvio-lacustrine environment at Yellowknife Bay, Gale crater, Mars. Science 343. https://doi.org/10.1126/science.1242777, 1242777–1242777.

Haberle, R.M., Clancy, R.T., Forget, F., Smith, M.D., Zurek, R.W., et al., 2017. The Atmosphere and Climate of Mars. Cambridge University Press.

Holmes, J.A., Patel, M.R., Lewis, S.R., 2017. The vertical transport of methane from different potential emission types on Mars: VERTICAL TRANSPORT OF METHANE ON MARS. Geophys. Res. Lett. 44, 8611–8620. https://doi.org/10.1002/2017GL074613.

Knak Jensen, S.J., Skibsted, J., Jakobsen, H.J., ten Kate, I.L., Gunnlaugsson, H.P., et al., 2014. A sink for methane on Mars? The answer is blowing in the wind. Icarus 236, 24–27. https://doi.org/10.1016/j.icarus.2014.03.036.

Korablev, O., Montmessin, F., Fedorova, A.A., Trokhimovskiy, A., Forget, F., et al., 2019. No detection of methane on Mars from early ExoMars trace gas orbiter observations. Nature 568, 517–520. https://doi.org/10.1038/s41586-019-1096-4.

Krasnopolsky, V.A., 2006. Some problems related to the origin of methane on Mars. Icarus 180, 359–367. https://doi.org/10.1016/j.icarus.2005.10.015.

Krasnopolsky, V.A., 2007. Long-term spectroscopic observations of Mars using IRTF/CSHELL: mapping of O2 dayglow, CO, and search for CH4. Icarus 190, 93–102. https://doi.org/10.1016/j.icarus.2007.02.014.

Krasnopolsky, V.A., 2012. Search for methane and upper limits to ethane and SO2 on Mars. Icarus 217, 144–152. https://doi.org/10.1016/j.icarus.2011.10.019.
Krasnopolsky, V.A., Bjoraker, G.L., Mumma, M.J., Jennings, D.E., 1997. High-resolution spectroscopy of Mars at 3.7 and 8 μm: A sensitive search for H_2O_2, H_2CO, HCl, and CH_4, and detection of HDO. J. Geophys. Res. Planets 102, 6525–6534. https://doi.org/10.1029/96JE03766.
Krasnopolsky, V.A., Maillard, J.P., Owen, T.C., 2004. Detection of methane in the martian atmosphere: evidence for life? Icarus 172, 537–547. https://doi.org/10.1016/j.icarus.2004.07.004.
Lefèvre, F., 2019. The enigma of methane on Mars. In: Cavalazzi, B., Westall, F. (Eds.), Biosignatures for Astrobiology, Advances in Astrobiology and Biogeophysics. Springer International Publishing, Cham, pp. 253–266. https://doi.org/10.1007/978-3-319-96175-0_12.
Lefèvre, F., Forget, F., 2009. Observed variations of methane on Mars unexplained by known atmospheric chemistry and physics. Nature 460, 720–723. https://doi.org/10.1038/nature08228.
Lellouch, E., Encrenaz, T., de Graauw, T., Erard, S., Morris, P., et al., 2000. The 2.4–spectrum of Mars observed with the infrared space observatory. Planet. Space Sci. 48, 1393–1405. https://doi.org/10.1016/S0032-0633(00)00118-5.
Liuzzi, G., Masiello, G., Serio, C., Venafra, S., Camy-Peyret, C., 2016. Physical inversion of the full IASI spectra: assessment of atmospheric parameters retrievals, consistency of spectroscopy and forward modelling. J. Quant. Spectrosc. Radiat. Transf. 182, 128–157. https://doi.org/10.1016/j.jqsrt.2016.05.022.
Liuzzi, G., Villanueva, G.L., Mumma, M.J., Smith, M.D., Daerden, F., et al., 2019. Methane on Mars: new insights into the sensitivity of CH4 with the NOMAD/ExoMars spectrometer through its first in-flight calibration. Icarus 321, 671–690. https://doi.org/10.1016/j.icarus.2018.09.021.
Liuzzi, G., Villanueva, G.L., Crismani, M.M.J., Smith, M.D., Mumma, M.J., et al., 2020. Strong variability of martian water ice clouds during dust storms revealed from exomars trace Gas Orbiter/NOMAD. J. Geophys. Res. Planets 125. https://doi.org/10.1029/2019JE006250.
Lyons, J.R., 2005. Formation of methane on Mars by fluid-rock interaction in the crust. Geophys. Res. Lett. 32, L13201 https://doi.org/10.1029/2004GL022161.
Maguire, W.C., 1977. Martian isotopic ratios and upper limits for possible minor constituents as derived from mariner 9 infrared spectrometer data. Icarus 32, 85–97. https://doi.org/10.1016/0019-1035(77)90051-3.
Mangold, N., Baratoux, D., Witasse, O., Encrenaz, T., Sotin, C., 2016. Mars: a small terrestrial planet. Astron. Astrophys. Rev. 24, 15. https://doi.org/10.1007/s00159-016-0099-5.
Moores, J.E., Schuerger, A.C., 2012. UV degradation of accreted organics on Mars: IDP longevity, surface reservoir of organics, and relevance to the detection of methane in the atmosphere: ORGANIC IDP SURFACE CARBON ON MARS. J. Geophys. Res. Planets 117. https://doi.org/10.1029/2012JE004060 n/a-n/a.
Moores, J.E., Gough, R.V., Martinez, G.M., Meslin, P.-Y., Smith, C.L., et al., 2019a. Methane seasonal cycle at Gale crater on Mars consistent with regolith adsorption and diffusion. Nat. Geosci. 12, 321–325. https://doi.org/10.1038/s41561-019-0313-y.
Moores, J.E., King, P.L., Smith, C.L., Martinez, G.M., Newman, C.E., et al., 2019b. The methane diurnal variation and microseepage flux at Gale crater, Mars as constrained by the ExoMars trace gas orbiter and curiosity observations. Geophys. Res. Lett. 46, 9430–9438. https://doi.org/10.1029/2019GL083800.
Mumma, M.J., Novak, R.E., Bonev, B.P., DiSanti, M.A., 2003. A sensitive search for methane on Mars. Presented at the American Astronomical Society. Bull. Am. Astron. Soc. 35, 14–18.
Mumma, M.J., Villanueva, G.L., Novak, R.E., Hewagama, T., Bonev, B.P., et al., 2009. Strong release of methane on Mars in northern summer 2003. Science 323, 1041–1045. https://doi.org/10.1126/science.1165243.
Neefs, E., Vandaele, A.C., Drummond, R., Thomas, I.R., Berkenbosch, S., et al., 2015. NOMAD spectrometer on the ExoMars trace gas orbiter mission: part 1—design, manufacturing and testing of the infrared channels. Appl. Opt. 54, 8494. https://doi.org/10.1364/AO.54.008494.
Oehler, D.Z., Etiope, G., 2017. Methane seepage on Mars: where to look and why. Astrobiology 17, 1233–1264. https://doi.org/10.1089/ast.2017.1657.
Olsen, K.S., Lefèvre, F., Montmessin, F., Trokhimovskiy, A., Baggio, L., et al., 2020. First detection of ozone in the mid-infrared at Mars: implications for methane detection. Astron. Astrophys. 639, A141. https://doi.org/10.1051/0004-6361/202038125.
Rodgers, C.D., 2000. Inverse Methods for Atmospheric Sounding: Series on Atmospheric, Oceanic and Planetary Physics. World Scientific Publishing Co. Pte. Ltd.
Roos-Serote, M., Atreya, S.K., Webster, C.R., Mahaffy, P.R., 2016. Cometary origin of atmospheric methane variations on Mars unlikely: METHANE ON MARS AND COMETS UNCORRELATED. J. Geophys. Res. Planets 121, 2108–2119. https://doi.org/10.1002/2016JE005076.
Segura, A., Navarro-González, R., 2005. Production of low molecular weight hydrocarbons by volcanic eruptions on early Mars. Orig. Life Evol. Biosph. 35, 477–487. https://doi.org/10.1007/s11084-005-6420-3.
Smith, M.D., 2008. Spacecraft observations of the Martian atmosphere. Annu. Rev. Earth Planet. Sci. 36, 191–219. https://doi.org/10.1146/annurev.earth.36.031207.124334.
Smith, M.D., 2019. THEMIS observations of the 2018 Mars global dust storm. J. Geophys. Res. Planets 124, 2929–2944. https://doi.org/10.1029/2019JE006107.
Summers, M.E., Lieb, B.J., Chapman, E., Yung, Y.L., 2002. Atmospheric biomarkers of subsurface life on Mars: ATMOSPHERIC BIOMARKERS ON MARS. Geophys. Res. Lett. 29 https://doi.org/10.1029/2002GL015377, 24–1–24–4.
Thomas, I.R., Vandaele, A.C., Robert, S., Neefs, E., Drummond, R., et al., 2016. Optical and radiometric models of the NOMAD instrument part II: the infrared channels - SO and LNO. Opt. Express 24, 3790. https://doi.org/10.1364/OE.24.003790.
Trokhimovskiy, A., Perevalov, V., Korablev, O., Fedorova, A.F., Olsen, K.S., et al., 2020. First observation of the magnetic dipole CO_2 absorption band at 3.3 μ m in the atmosphere of Mars by the ExoMars trace gas orbiter ACS instrument. Astron. Astrophys. 639, A142. https://doi.org/10.1051/0004-6361/202038134.
Vandaele, A.C., Neefs, E., Drummond, R., Thomas, I.R., Daerden, F., et al., 2015. Science objectives and performances of NOMAD, a spectrometer suite for the ExoMars TGO mission. Planet. Space Sci. 119, 233–249. https://doi.org/10.1016/j.pss.2015.10.003.
Vandaele, A.C., Lopez-Moreno, J.-J., Patel, M.R., Bellucci, G., Daerden, F., et al., 2018. NOMAD, an integrated suite of three spectrometers for the ExoMars trace gas Mission: technical description, science objectives and expected performance. Space Sci. Rev. 214, 80. https://doi.org/10.1007/s11214-018-0517-2.
Vandaele, A.C., Korablev, O., Daerden, F., Aoki, S., Thomas, I.R., et al., 2019. Martian dust storm impact on atmospheric H2O and D/H observed by ExoMars trace gas orbiter. Nature 568, 521–525. https://doi.org/10.1038/s41586-019-1097-3.
Villanueva, G.L., Mumma, M.J., Novak, R.E., Radeva, Y.L., Käufl, H.U., et al., 2013. A sensitive search for organics (CH4, CH3OH, H2CO, C2H6, C2H2, C2H4), hydroperoxyl (HO2), nitrogen compounds (N2O, NH3, HCN) and chlorine species (HCl, CH3Cl) on Mars using ground-based high-resolution infrared spectroscopy. Icarus 223, 11–27. https://doi.org/10.1016/j.icarus.2012.11.013.
Villanueva, G.L., Smith, M.D., Protopapa, S., Faggi, S., Mandell, A.M., 2018. Planetary Spectrum generator: an accurate online radiative transfer suite for atmospheres, comets, small bodies and exoplanets. J. Quant. Spectrosc. Radiat. Transf. 217, 86–104. https://doi.org/10.1016/j.jqsrt.2018.05.023.
Villanueva, G.L., Liuzzi, G., Crismani, M.M.J., Aoki, S., Vandaele, A.C., et al., 2020. Strong isotopic fractionation observed in the Martian atmosphere with ExoMars/NOMAD. Sci. Adv.
Viscardy, S., Daerden, F., Neary, L., 2016. Formation of layers of methane in the atmosphere of Mars after surface release: FORMATION OF LAYERS OF METHANE ON MARS. Geophys. Res. Lett. 43, 1868–1875. https://doi.org/10.1002/2015GL067443.
Waugh, D.W., Toigo, A.D., Guzewich, S.D., 2019. Age of martian air: time scales for martian atmospheric transport. Icarus 317, 148–157. https://doi.org/10.1016/j.icarus.2018.08.002.
Webster, C.R., Mahaffy, P.R., 2011. Determining the local abundance of Martian methane and its' 13C/12C and D/H isotopic ratios for comparison with related gas and soil analysis on the 2011 Mars science laboratory (MSL) mission. Planet. Space Sci. 59, 271–283. https://doi.org/10.1016/j.pss.2010.08.021.
Webster, C.R., Mahaffy, P.R., Atreya, S.K., Flesch, G.J., Farley, K.A., et al., 2013. Low upper limit to methane abundance on Mars. Science 342, 355–357. https://doi.org/10.1126/science.1242902.
Webster, C.R., Mahaffy, P.R., Atreya, S.K., Flesch, G.J., Mischna, M.A., et al., 2015. Mars methane detection and variability at Gale crater. Science 347, 415–417. https://doi.org/10.1126/science.1261713.
Webster, C.R., Mahaffy, P.R., Atreya, S.K., Moores, J.E., Flesch, G.J., et al., 2018. Background levels of methane in Mars' atmosphere show strong seasonal variations. Science 360, 1093–1096. https://doi.org/10.1126/science.aaq0131.
Webster, C.R., Mahaffy, P.R., Atreya, S.K., Flesch, G.J., Malespin, C.A., et al., 2020. Curiosity Mars methane measurements are not confused by ozone. Astron. Astrophys. 641, L3. https://doi.org/10.1051/0004-6361/202038815.
Wong, A.-S., 2003. Chemical markers of possible hot spots on Mars. J. Geophys. Res. 108, 5026. https://doi.org/10.1029/2002JE002003.
Yung, Y.L., Chen, P., Nealson, K., Atreya, S., Beckett, P., et al., 2018. Methane on Mars and habitability: challenges and responses. Astrobiology 18, 1221–1242. https://doi.org/10.1089/ast.2018.1917.
Zahnle, K., 2015. Play it again, SAM. Science 347, 370–371. https://doi.org/10.1126/science.aaa3687.
Zahnle, K., Freedman, R.S., Catling, D.C., 2011. Is there methane on Mars? Icarus 212, 493–503. https://doi.org/10.1016/j.icarus.2010.11.027.